Journal of the European Ceramic Society **6** (1990) 369–374

Weakest-link Failure Predictions for Ceramics Using Finite Element Post-processing

L. J. M. G. Dortmans & G. de With*

Centre for Technical Ceramics, P.O. Box 595, 5600 AN Eindhoven, The Netherlands

(Received 17 April 1990; revised version received 7 June 1990; accepted 22 June 1990)

Abstract

Weakest-link failure prediction models according to Weibull, Stanley and Lamon have been implemented in a post-processing program supplementing a finite element modelling code. Failure predictions for equi-biaxial loading from uniaxial bending test data reveal significant differences between the various formulations. The choice of a particular failure model for a particular material therefore has to be validated by additional information, e.g. by fractography or micrography.

Modelle zur Vorhersage des Versagens nach dem Prinzip des größten Fehlers gemäß Weibull, Stanely und Lamon wurden zur Ergänzung eines Finite-Elemente-Verfahrens in der Qualitätskontrolle herangezogen. Versagensvorhersagen für gleichmäßige zweiachsige Belastung aus uniaxialen Biegeversuchsdaten zeigten zwischen den verschiedenen Modellen beträchtliche Unterschiede. Die Wahl eines bestimmten Versagensmodells für ein bestimmtes Material muß daher durch zusätzliche Informationen, wie z.B. Fraktographie und Mikroskopie verifiziert werden.

On a réalisé l'implentation de modèles de prévision de rupture par maillon le plus faible selon Weibull, Stanley et Lamon dans un programme post-opératoire complétant un code de modèlisation par éléments finis. Les valeurs exprimant les prévisions de rupture en chargement equi-biaxial obteunes par essai en flexion uniaxiale sont sensiblement différentes selon la formule utilisée. Le choix d'un modèle de rupture particulier pour un matériau donné doit donc être complété par des informations complémentaires obtenues, par exemple par fractographie ou micrographie.

1 Introduction

The determination of the probability of failure of brittle ceramic components is the object of both experimental and theoretical studies. Usually a weakest-link model is applied with parameters determined from experimental data. A number of examples of the application of the well-known models of Weibull, Stanley and Lamon (amongst others) have been described in literature.[1–8] Test methods to gather experimental data are the three- and four-point bend tests, the tensile test, the ball-on-ring biaxial bending test, etc.[6,8,9] Ideally, the parameters determined from one particular test should allow the use of the model in situations with a different geometry and/or a different stress state. However, the occurrence of multiple defect types does not always allow this type of extrapolation. The criticality of a particular defect can depend upon the stress state a component is subjected to. Moreover, it may be necessary to distinguish between different types of defects, which have their own statistical distribution,[8] e.g. volume and surface defects. In order to be able to study the failure probability of a ceramic component, with arbitrary geometry and stress state, a computer code was developed dealing with the weakest-link models as proposed by Weibull, Stanley and Lamon. The main objective was to obtain a tool for the comparison of the predictions of these models. In this paper some aspects of the computer program are discussed. In addition an example of its application is given in an evaluation of the predictions of the models mentioned above for the biaxial ball-on-ring test with material data taken from uniaxial experiments.

* Also affiliated with Philips Research Laboratories, PO Box 80000, 5600 JA Eindhoven, The Netherlands.

Journal of the European Ceramic Society 0955-2219/90/$3.50

2 Weakest-link Failure Probability Models

The models of Weibull, Stanley and Lamon were taken as the starting point in the development of the computer program. Other models can easily be entered in the current version of the program if necessary. The models of Weibull, Stanley and Lamon are derived from a weakest-link principle:

$$\Delta P_f = 1 - \exp\{-\int g(S)\,dS\} \tag{1}$$

where ΔP_f denotes the failure probability for a small homogeneously stressed volume or surface element. The integrand $g(S)\,dS$ is the number of defects with strengths between S and $S + dS$. According to the weakest-link principle, for the entire component considered, relation (1) yields:

$$P_f^V = 1 - \exp\left\{-\int_V \left[\int g^V(S)\,dS\right] dV\right\} \tag{2}$$

$$P_f^A = 1 - \exp\left\{-\int_A \left[\int g^A(S)\,dS\right] dA\right\} \tag{3}$$

where P_f^V and P_f^A denote the failure probability due to volume and surface defects, respectively.

Assuming only one defect type for the volume and the surface of a component for the models of Weibull, Stanley and Lamon, relations (2) and (3) can be elaborated for the case of an isotropic defect distribution. The resulting equations can be written most conveniently in the four-parameter notation introduced by Stanley *et al.*:[3]

$$P_f^V = 1 - \exp\left\{-\left(\frac{1}{m}!\right)^m \frac{V}{V_u}\left(\frac{S_{nom}}{S_u}\right)^m \Sigma(V)\right\} \tag{4}$$

$$P_f^A = 1 - \exp\left\{-\left(\frac{1}{m}!\right)^m \frac{A}{A_u}\left(\frac{S_{nom}}{S_u}\right)^m \Sigma(A)\right\} \tag{5}$$

where m is the Weibull modulus, S_{nom} a given nominal or reference stress, S_u the strength per unit volume $V_u = 1$ or unit surface $A_u = 1$. The values of m, S_{nom} and S_u may be different for volume and surface defects. $\Sigma(V)$ and $\Sigma(A)$ are the so-called stress–volume and stress–surface integrals, respectively. Denoting the principal stresses with S_1, S_2 and S_3 ($S_1 \geq S_2 \geq S_3$), the expressions for $\Sigma(V)$ and $\Sigma(A)$ for the failure probability models can be written as follows:

Model of Weibull (normal stress criterium)

$$\Sigma(V) = \frac{1}{V}\int_V \left(\frac{S_1}{S_{nom}}\right)^m \left[\frac{1}{4\pi}\int_{B_u} g^m\,dB_u\right] dV \tag{6}$$

$$\Sigma(A) = \frac{1}{A}\int_A \left(\frac{S_1}{S_{nom}}\right)^m \left[\frac{1}{4\pi}\int_{B_u} g^m\,dB_u\right] dA \tag{7}$$

$$g = \underset{\sim}{n}^T \hat{\underset{\sim}{S}}\,\underset{\sim}{n} \tag{8}$$

$$\hat{\underset{\sim}{S}} = \begin{vmatrix} 1 & 0 & 0 \\ 0 & S_2/S_1 & 0 \\ 0 & 0 & S_3/S_1 \end{vmatrix} \qquad \underset{\sim}{n}^T = [n_1 n_2 n_3] \tag{9}$$

where B_u is the surface of a sphere with radius 1 and unit outward normal $\underset{\sim}{n}$.

Model of Stanley (independent stress criterium)

$$\Sigma(V) = \frac{1}{V}\int_V \left[\left(\frac{S_1}{H_1 S_{nom}}\right)^m + \left(\frac{S_2}{H_2 S_{nom}}\right)^m + \left(\frac{S_3}{H_3 S_{nom}}\right)^m\right] dV \tag{10}$$

$$\Sigma(A) = \frac{1}{A}\int_A \left[\left(\frac{S_1}{H_1 S_{nom}}\right)^m + \left(\frac{S_2}{H_2 S_{nom}}\right)^m + \left(\frac{S_3}{H_3 S_{nom}}\right)^m\right] dA \tag{11}$$

where H_1, H_2 and H_3 are weight factors.

Model of Lamon (maximum strain energy release rate criterium)

$$\Sigma(V) = \frac{1}{V}\int_V \left(\frac{S_1}{S_{nom}}\right)^m \left[\frac{1}{4\pi}\int_{B_u} h^m\,dB_u\right] dV \tag{12}$$

$$\Sigma(A) = \frac{1}{A}\int_A \left(\frac{S_1}{S_{nom}}\right)^m \left[\frac{1}{4\pi}\int_{B_u} h^m\,dB_u\right] dA \tag{13}$$

$$h^4 = (\underset{\sim}{n}^T \hat{\underset{\sim}{S}}^2 \underset{\sim}{n})^2 + 4(\underset{\sim}{n}^T \hat{\underset{\sim}{S}}^2 \underset{\sim}{n})(\underset{\sim}{n}^T \hat{\underset{\sim}{S}}\,\underset{\sim}{n})^2 - 4(\underset{\sim}{n}^T \hat{\underset{\sim}{S}}\,\underset{\sim}{n})^4 \tag{14}$$

Relations (4)–(14) served as a starting point for the development of the computer program discussed in Section 3.

3 FAILUR: A Post-processor for Failure Probability Calculations

3.1 General aspects

Evaluation of the relations given in Section 2 by analytical means is only possible for a limited number of (thermo-)mechanical problems. However, as indicated by Stanley, Lamon and Gyenkeyesi (amongst others),[3,7,10] a more general tool can be developed, making use of the results of a finite element package. Using the stresses calculated at element level, the integrals given in Section 2 can be evaluated easily and with sufficient accuracy. Therefore a computer program, or more precisely, a post-processor was written (in Fortran-77), which uses the output of the finite element package

SYSTUS.[11] The relations given in Section 2 have been implemented for two-dimensional (plane stress, plane strain and axisymmetric) and three-dimensional (bricks, tetrahedra) elements. FAILUR produces the failure probability of the component with user-defined values for material parameters like m, S_u, etc. As pointed out by Stanley & Chan[5] the failure probability cannot increase with decreasing stress. Therefore FAILUR incorporates an option to keep the failure probability at a Gauss point of an element constant at the value for the highest applied stresses in the case the stresses decrease.

For the evaluation of the stress-integrals the stresses at the Gauss points of the elements are used, as this has proven to yield more accurate results compared to the stresses at the centroid of the element.[12]

3.2 Analysis of the four-point bend test

In order to illustrate the use of FAILUR and to pay attention to some important aspects for practical calculations, the four-point bend test will be discussed (Fig. 1).

For a specimen with dimensions length × width × height = $l \times b \times h$, such that the stress field can be considered as uniaxial, the expressions for the stress integrals given in Section 2 for the model of Stanley reduce to:[4]

Model of Stanley

$$\Sigma^S(V) = \frac{m+2}{4(m+1)^2}$$
$$\Sigma^S(A) = \frac{m+2}{4(m+1)^2}\left(1 + \frac{m}{1+h/b}\right) \tag{15}$$

Similarly for the models of Weibull and Lamon one can derive:

Model of Weibull

$$\Sigma^W(V) = \Sigma^S(V) I^W(m) \qquad \Sigma^W(A) = \Sigma^S(A) I^W(m) \tag{16}$$

$$I^W(m) = \int_0^{\pi/2} \cos^{2m}\alpha \sin\alpha \, d\alpha = \frac{1}{2m+1} \tag{17}$$

Model of Lamon

$$\Sigma^L(V) = \Sigma^S(V) I^L(m) \qquad \Sigma^L(A) = \Sigma^S(A) I^L(m) \tag{18}$$

$$I^L(m) = \int_0^{\pi/2} (1 + \sin^2 2\alpha)^{m/4} \cos^m\alpha \sin\alpha \, d\alpha \tag{19}$$

From relations (4), (5) and (15) to (19) it is readily found that the models considered yield the same prediction for the failure probabilities for the four-point bend test if the unit strength S_u for the various

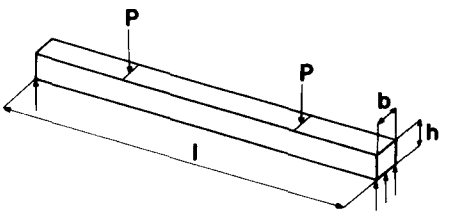

Fig. 1. The four-point bend test with specimen dimensions length × width × height $l \times b \times h$.

models meets the following conditions for both volume and surface defects:

$$(S_u)^L = (S_u)^S (I^L(m))^{1/m} \tag{20}$$

$$(S_u)^W = (S_u)^S (I^W(m))^{1/m} \tag{21}$$

and if the moduli m are identical for all models ($(S_u)^S$ is the unit strength for the model of Stanley, etc.). In the remainder of this paper it will be assumed that the parameters in the various models satisfy these conditions and that they are identical for both volume and surface defects (which merely simplifies the analysis, but is not essential). Assuming that $(S_u)^S$ has a value of 200 N/mm^2, elaboration of relations (20) and (21) yields the required combinations of material parameters given in Table 1 for $m = 5$, 10 and 20. With the parameters given in Table 1, the models of Stanley, Weibull and Lamon give the same results if an uniaxial stress field is assumed. A more detailed analysis may show differences as shear stresses will also be present. Here the finite element method can be a useful tool. With the mesh shown in Fig. 2 a plane stress analysis was carried out. The mesh contains 224 eight-node isoparametric volume elements (to model volume defects) and 64 three-node isoparametric surface (skin) elements (to model surface defects). Note that only half the specimen needs to be modelled because of its symmetry. The following parameter values were chosen:

$l = 50$ mm $\quad b = 4{\cdot}5$ mm $\quad h = 3{\cdot}5$ mm
$V = 787{\cdot}50$ mm^3 $\quad A = 831{\cdot}50$ mm^2
$E = 58{\cdot}6$ GPa $\quad \nu = 0{\cdot}22$
$S_{nom} = 136{\cdot}05$ N/mm^2 (maximum tensile stress according to the theory with uniaxial stress field)
$H_1 = H_2 = H_3 = -8$

Table 1. Required combinations of material parameters for $(S_u)^S = 200$ N/mm^2

m	$(l/m)!$	$I^W(m)$	$I^L(m)$	$(S_u)^W$	$(S_u)^L$
5	0·918 2	0·090 9	0·301 6	123·8	157·4
10	0·951 3	0·047 6	0·249 3	147·5	174·1
20	0·973 5	0·024 4	0·236 7	166·1	186·1

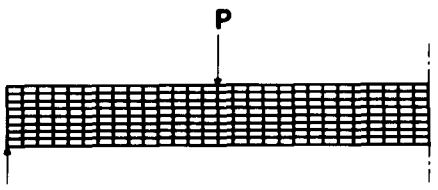

Fig. 2. Finite element mesh for plane stress analysis of the four-point bend test.

As an example of the results obtained with SYSTUS and FAILUR in Table 2 the theoretical values for the stress–volume and stress–surface integrals (relations (15) to (19)) are compared with the numerical values.

As was to be expected the calculated results for the stress integrals agree well with the theoretical values. The differences found can be caused by the following:

(1) The finite element method yields a non-uniaxial stress field in contrast to the theoretical analysis. As the shear stresses are small (typically an order of magnitude $(h/l)^2$ smaller than the bending stresses), their influence is of minor importance.
(2) All necessary integrations are done numerically leading to small errors, which may be neglected, however.
(3) The finite element method yields an approximation of the stresses. Better accuracy for both the stresses and the stress integrals is generally obtained by mesh refinement. This aspect will be considered further hereafter.

To analyse the influence of mesh refinement, the mesh shown in Fig. 2 ('fine mesh') was modified by taking only half the number of elements for the height of the specimen ('coarse mesh'). To illustrate the influence of this modification, Table 3 shows the stress–volume integrals for the model of Stanley for $m = 5$, 10 and 20. Clearly for higher values of m, a coarse mesh yields poor results for the stress integrals (and the failure probabilities). Use of a sufficiently fine mesh is therefore indispensable. The same holds when applying lower order elements (e.g. four-node elements instead of eight-node elements). As is generally accepted with lower-order elements a finer mesh is required to achieve accurate results.

Table 3. The relative errors in the calculated stress–volume integrals for the model of Stanley for coarse and fine meshes

Errors	*Coarse mesh*	*Fine mesh*
$\Sigma(V)$ $m = 5$	−0·16	0·36
$m = 10$	−7·57	0·15
$m = 20$	−43·08	−6·23

4 Prediction of Biaxial from Uniaxial Strength Data

To illustrate the use of the program FAILUR (Section 3) and to investigate the influence of the choice of a particular failure model, some calculations have been carried out which will be described in this section. The starting point for these calculations are the material parameters given in Section 3, which were chosen such that the models of Weibull, Stanley and Lamon yield the same prediction for the four-point bend test. A straightforward analysis will show that this is also true for the three-point bend test. These parameters can now be used to calculate the failure probability of a specimen in the ball-on-ring biaxial bend test. The ball-on-ring bend test has been described in detail by de With *et al.*[9] As shown in Fig. 3, a circular plate with radius R is loaded centrally with a force F. The plate is supported at a radius a. It has been shown[9] that the force F can be replaced by a uniform pressure p

$$p = \frac{F}{\pi b^2}$$

Table 2. The theoretical values for the stress integrals for the models of Weibull, Stanley and Lamon and the relative errors in the calculated values ((calculated − theoretical)/theoretical × 100%)

	$\Sigma(V)$				$\Sigma(A)$		
	$m = 5$	$m = 10$	$m = 20$		$m = 5$	$m = 10$	$m = 20$
Theory				Theory			
Weibull	0·004 4	0·001 2	0·000 3	Weibull	0·016 8	0·007 8	0·003 7
Lamon	0·014 7	0·006 2	0·002 9	Lamon	0·055 9	0·040 9	0·036 2
Stanley	0·048 6	0·024 8	0·012 5	Stanley	0·185 3	0·164 3	0·152 8
Errors				Errors			
Weibull	0·34	0·13	−5·81	Weibull	−2·86	−2·35	−0·96
Lamon	0·38	0·17	−6·24	Lamon	−2·86	−2·39	−1·43
Stanley	0·36	0·15	−6·23	Stanley	−0·00	−0·88	−1·39

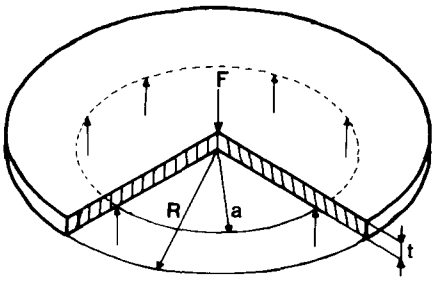

Fig. 3. The ball-on-ring biaxial bend test. R = specimen radius, a = support radius, t = specimen thickness.

where b is the radius of the circle the pressure acts on. The value of b can safely be taken as

$$b = \frac{t}{3}$$

with t as the plate thickness. The maximum tangential and radial stresses are found at the centre of the plate and are equal to:

$$S_{nom} = \frac{3F(1+\nu)}{4\pi t^2}\left[1 + 2\ln\left(\frac{a}{b}\right) + \frac{(1-\nu)}{(1+\nu)}\frac{a^2}{R^2}\left\{1 - \frac{b^2}{2a^2}\right\}\right] \quad (22)$$

where ν is Poisson's ratio of the specimen. For the calculations discussed in the remainder of this paper, the following parameter values were chosen:

$R = 15\,\text{mm}$ $a = 10\,\text{mm}$ $t = 1{\cdot}5\,\text{mm}$
$b = 0{\cdot}5\,\text{mm}$ $E = 58{\cdot}6\,\text{GPa}$ $\nu = 0{\cdot}22$

The stresses in the specimen were calculated using the axisymmetric mesh given in Fig. 4, which contains 410 eight-node isoparametric elements to describe the volume and 92 three-node isoparametric skin-elements describing the surface of the specimen. With FAILUR the stress-integrals and the failure probability due to both volume and surface defects (which were assumed to have the same modulus m and unit strength S_u) were calculated. As in this case the stress-integrals do not depend upon the nominal stress S_{nom}, one stress calculation suffices to be able to generate the familiar Weibull-plot using eqns (4) and (5). As a typical example of the outcome of the calculations in Fig. 5

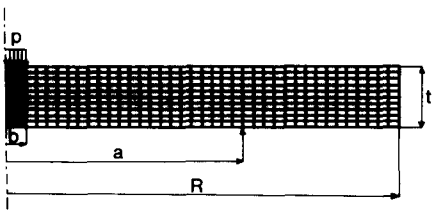

Fig. 4. Finite element mesh for axisymmetric stress analysis of the ball-on-ring bend test.

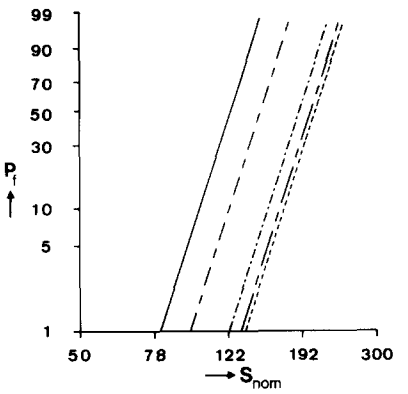

Fig. 5. Weibull plot for surface defects with $m = 10$. ———, Four-point bend test; – – – –, three-point bend test; – · – · –, prediction model for Weibull biaxial bend test; ——— · ———, prediction model of Lamon biaxial bend test; – – – – –, prediction model of Stanley biaxial bend test.

the results for surface defects for a modulus $m = 10$ are given. Clearly the probability of failure for the ball-on-ring test (at the same nominal stress) is much smaller than for the three- and four-point bend test. It is remarkable, however, that the predictions for the models of Weibull, Stanley and Lamon show a marked difference for the ball-on-ring test, although they predict the same values for the three- and four-point bend test.

This can further be illustrated by considering the mean nominal fracture stress $\bar{S}_{nom}$ which is defined by

$$\bar{S}_{nom} = \int_0^\infty \frac{dP_f}{dS_{nom}} S_{nom}\, dS_{nom} \quad (23)$$

For volume defects use of relation (4) yields

$$\bar{S}_{nom} = S_u\left(\frac{V_u}{V\Sigma(V)}\right)^{1/m} \quad (24)$$

The predicted values for the various tests for volume defects are given in Fig. 6. It is clearly observed that the predictions for the biaxial bend test for the

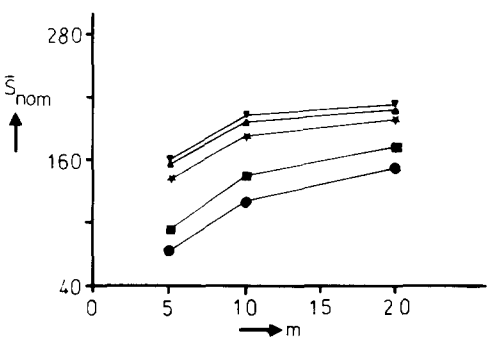

Fig. 6. The values for the mean nominal fracture stress $\bar{S}_{nom}$ for volume defects as a function of m. ●, Four-point bend test; ■, three-point bend test; ×, prediction model of Weibull biaxial bend test; ▼, prediction model of Lamon biaxial bend test; ▲, prediction model of Stanley biaxial bend test.

models of Stanley, Weibull and Lamon show differences of about 10% although they predict the same values for the three- and four-point bend test. Although these differences may seem rather small, it must be recognized that these small differences may lead to far larger differences in the predicted failure probabilities. This is easily demonstrated considering relations (4), (5) and (24):

$$P_f = 1 - \exp\left\{-\left(\frac{1}{m}!\right)^m \left(\frac{S_{nom}}{\bar{S}_{nom}}\right)^m\right\} \qquad (25)$$

When P_f is small ($\ln(1-P_f) \approx -P_f$), for the same stress S_{nom} the failure probabilities P_1 and P_2 of these two models, given their respective mean nominal fracture stress S_1 and S_2, are related by:

$$\frac{P_2}{P_1} \approx \left(\frac{S_1}{S_2}\right)^m \qquad (26)$$

If $S_1 \approx 0{\cdot}9S_2$ (as mentioned above) for a value of $m = 10$, $P_1 \approx 2{\cdot}87P_2$ and for $m = 20$, $P_1 \approx 8{\cdot}22P_2$. This shows that the magnitude of the differences in the failure probabilities may greatly exceed the magnitude of the differences in the values for the mean nominal fracture stress. Hence the extrapolation of uniaxial to biaxial strength data strongly depends upon the failure model selected (and also *vice versa*, of course). Validation of a particular weakest-link model for a particular ceramic component is therefore a necessity for reliable failure prediction.

5 Concluding Remarks

The calculation of the probability of failure of ceramic components using finite element modelling has been implemented in a post-processor. Different failure models for both volume and surface defects can be applied. As has been shown in the example in Section 4, the values for the mean nominal fracture stress predicted by the various models may differ only little. However, the failure probabilities predicted by the various models may differ significantly, especially for the lower stress range, which is of major interest for practical design purposes.

With this numerical tool experimentally obtained strength data can be analysed to obtain an indication about the validity of a particular failure model for a certain ceramic material. As has been shown in the example in Section 4 such a validation is necessary if strength data are to be extrapolated from one test to another. Whether such a validation yields acceptable results is not only a matter of experimental accuracy, but it is also influenced by the possible occurrence of multiple defect types which have to be detected and accounted for. Microstructural analyses therefore have an important role in this validation process. Continuing research at the Centre for Technical Ceramics aims at such a validation process in which experimental results are being gathered and analysed with the numerical tool described here.

Acknowledgement

This work has partly been supported by the Commission for the Innovative Research Program Technical Ceramics (IOP-TK) of the Ministry of Economic Affairs in the Netherlands (IOP-TK research grant 88.B040).

References

1. Weibull, W., A statistical distribution function of wide applicability. *J. Appl. Mech.*, **18**(3) (1951) 293–7.
2. Stanley, P., Fessler, H. & Sevill, A. D., An engineer's approach to the prediction of failure probability of brittle components. *Proc. Brit. Ceram. Soc.*, **22** (1973) 453–87.
3. Stanley, P., Sivill, A. D. & Fessler, H., Applications of the four-function Weibull equation in the design of brittle components. In *Fracture Mechanics of Ceramics*, Vol. 3, ed. R. C. Bradt, D. P. H. Hasselman & F. F. Lange. Plenum, 1978, pp. 51–66.
4. Stanley, P., Sivill, A. D. & Fessler, H., The application and confirmation of a predictive technique for the fracture of brittle components. In *Proc. 5th Int. Conf. on Experimental Stress Analysis*, Udine, Italy, 1974.
5. Stanley, P. & Chau, F. S., A probabilistic treatment of brittle fracture under non-monotonically increasing stresses. *Int. J. Fracture*, **22** (1983) 187–202.
6. Stanley, P., Sivill, A. D. & Fessler, H., The unit strength concept in the interpretation of beam test results for brittle materials. *Proc. I. Mech. E.*, **190** (1976) 585–95.
7. Lamon, J., Ceramics reliability: Statistical analysis of multiaxial failure using the Weibull approach and the multiaxial elemental strength model. ASME Gas Turbine and Aeroengine Congress, Amsterdam, The Netherlands, 1988, ASME-88-GT-147.
8. Lamon, J. & Evans, A. G., Statistical analysis of bending strengths for brittle solids: A multiaxial fracture problem. *J. Am. Ceram. Soc.*, **66**(3) (1983) 177–82.
9. De With, G. & Wagemans, H. H. M., Ball-on-ring test revisited. *J. Am. Ceram. Soc.*, **72**(8) (1989) 1538–41.
10. Gyekenyesi, J. P. & Nemeth, N. N., Surface flaw reliability analysis of ceramic components with the Scare finite element postprocessor program. ASME Gas Turbine Conference and Exhibition, Anaheim, USA, 1987, ASME-87-GT-69.
11. SYSTUS, Finite element system TITUS user's manual. Framatome, Paris, France.
12. McLean, A. F. & Hartsock, D. L., Design with structural ceramics. In *Treatise on Material Science and Technology*, Vol. 29, *Structural Ceramics*, ed. J. B. Wachtman, Jr. Academic Press, New York, 1989, pp. 27–95.